Taylor & Francis
Taylor & Francis Group

AVIATION
ISSN 1648-7788 print / ISSN 1822-4180 online
2012 Volume 16(3): 76–83
doi:10.3846/16487788.2012.732320

MITIGATION OF SLIVERS USING A NEW PROPELLANT GRAIN DESIGN TO IMPROVE PROPULSION SYSTEMS

Sarah Farrukh[1], M. Bilal Khan[2]

School of Chemical and Materials Engineering, National University of Science and Technology, Islamabad, Pakistan
E-mails: [1]sarah@scme.nust.edu.pk (corresponding author), [2]bilalkhan-ccems@nust.edu.pk

Received 14 Mart 2012; acceped 20 July 2012

Sarah FARRUKH, *MSc*
Education: 2006– master's degree in Materials and Solid State Physics, Quaid-i-Azam University.
2010–MS degree in Propulsion and Energetic Materials, National University of Sciences and Technology.
Experience: researcher, National University of Sciences and Technology.
Research interests: propulsion systems, computational analysis of structures, polymeric membranes.

M. Bilal Khan, *Dr PhD*
Education: MS Chemical Engineering and Aerospace, University of Arizona.
PhD Polymer Engineering, Imperial College London.
Experience: researcher/professor, National University of Sciences and Technology.
Fields of research and teaching: reactive polymer composites, interface engineering, urethane systems, nano science and technology, propulsion systems, ablative materials, extrusion.

Abstract. The research work addresses mathematical modelling and computational analysis of novel solid propellant grain configuration. The aviation industry is working on propulsion systems as well. For high thrust in rockets, space ships, and even in aircraft, solid propellant grains can be used as fuel. Grain design is a vital and integral part of solid propellant design. The designer has many options available for selecting grain configuration. Several design parameters – volumetric loading fractions, web fraction, length to diameter ratio, and port area – are normally tailored to mission demands. The star grain configuration has been a mainstay in this industry since 1935. The star grain configuration does however have a long-standing drawback, namely the formation of slivers. In this paper we present a new grain configuration, the "rose petal", which overcomes the drawback of the traditional star grain design. The configuration is modelled using relevant internal ballistic relations. The design computation is executed in MATLAB. Thrust and time and burn area time curves are generated for a prescribed port area. Comparisons are drawn between the two configurations, clearly revealing that the new configuration obviates the occurrence of unwanted slivers otherwise generated in the old star design, which lowers the efficiency of all those propulsion systems in which solid propellants are used.

Keywords: rose petal grain, slivers, propulsion systems, port area, star grain, thrust curve, propellant configuration, aviation.

Copyright © 2012 Vilnius Gediminas Technical University (VGTU) Press Technika
http://www.tandfonline.com/TAVI

1. Introduction

Composite propellants are primary ingredients of solid propulsion systems. They have a resilient poly matrix containing an oxidizer that releases propulsive energy on ignition. Ammonium perchlorate (AP)-based composite propellants have been the workhorse in the field of solid rocket propulsion for more than 5 decades. This type of propellant typically contains a multi-modal distribution of solids embedded in hydroxyl-terminated polybutadiene (HTPB) matrix (Cai *et al.* 2008). Regardless of the composition, however, all propellants are processed into a similar basic geometric form, referred to as a propellant grain. Propellant grains are cylindrical in shape to fit neatly into a casing in order to maximise volumetric efficiency.

Two types of solid grain blocks are used in the space industry. These are cylindrical blocks with combustion at the end, or surface and cylindrical blocks with internal combustion. The so-called end burners produce constant thrust throughout the burn. In the latter type, the combustion surface evolves across the length of a central port. Most grains however are cast with a hollow core, burning from the inside out and are case bonded (Davenas 1993). A central core, surface area, and geometry that extend the full length of the grain are usually introduced to increase the propellant surface area. Grains are classified accordingly to the main orientation of burning.

The thrust profile over time is controlled by the grain geometry. The shape of the grain determines the particular type of mission it will perform. Geometrical consideration determines whether the thrust increases, decreases or stays constant. The thrust time curve, the desired burning time, motor mass, and volume are the primary design factors. The grain geometry is selected to fit these requirements. The grain should be designed so that it will utilise the maximum available volume in the chamber efficiently and produce a suitable burning surface with associated thrust time profile. An overriding requirement is that the amount of slivers should be minimal.

Grain configurations are classified according to their web fraction, L/D ratio and volumetric loading fraction. Some of most widely used two-dimensional grain configurations are end burning (EB), internal burning tube (IBTG), slotted tube grain (STG), and star grain (SG) (Sutton, Biblarz 2001).

A reasonably methodical procedure is followed in selecting and designing the specific grain geometry. Various grain geometries including two-dimensional and three-dimensional grains have been elaborated in this context (Barrere 1977). The prediction and analysis of burning profiles of various grains provide a great deal of information (Davenas, Thepenier 1999). The geometric parameters of star grain, their effects on internal ballistics, and their future trends provide better understanding regarding star grain (Ricciardi 1992). Many problems are solved by the simulation of solid propellants (Dick *et al* 2005). Wilcox used a minimum distance function (MDF) to simulate burning propellants (Wilcox *et al.* 2005). Stein mathematically modelled both star grain (SG) and internal burning tube grain (IBTG) and concluded that performance is enhanced with the merger of the two configurations (Stein 2008).

2. Material and methods

Two-dimensional mathematical modelling and computational analysis

In this paper we use the module presented in the layout of figure 1 for mathematical modelling and in subsequent computer analysis.

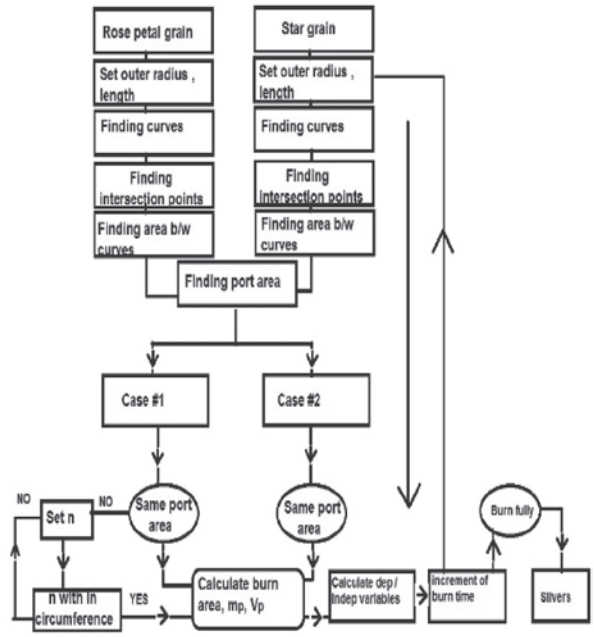

Fig. 1. Grain geometry and computational analysis module

2.1. Geometrical considerations

The traditional star grain and the proposed rose petal grain configuration appear in fig. 2.

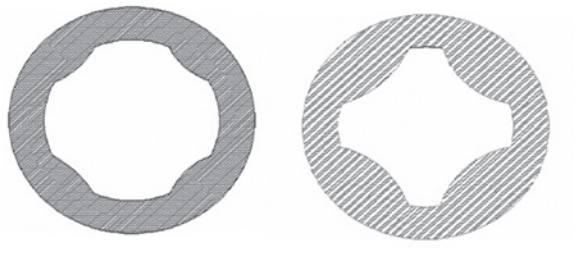

Fig. 2. Rose petal grain configuration (proposed) and star grain configuration (existing)

In this paper two cases have been considered for both configurations, keeping port areas constant. Thrust, burn area curves, sliver mass, and area of both configurations are investigated for constant port area. To find port area, we have to follow a calculation procedure as given below.

2.1.1. Determining curves

The two curve segments representing the respective grain geometry are indicated in fig. 3.

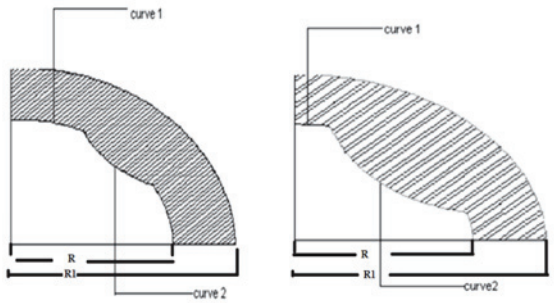

Fig. 3. First replicas of rose petal and star shape grain configuration

Curve 1 is a *circular curve* and curve 2 is an *a*(1/X) curve*. The equations of both curves are given below (Thomas, Finney 1995).

$Y^2 + X^2 = R^2$ (Simple circular curve eq.),

$a^*\left(\frac{1}{X}\right)$ (a is multiple).

2.1.2. Determining intersection points

In the second step, we find the intersection points where these curves meet. For this the following equations are applied.

$$Y^2 = R^2 - X^2, \tag{1}$$

$$Y = a^*\left(\frac{1}{X}\right). \tag{2}$$

After the mathematical operations, equation (1) and (2) are transformed thus.

$$y^2 - R^2 y + a = 0. \tag{3}$$

In equation (3), R and a are constants. These constants, being design constants, are set for each configuration. In this paper we discuss two different cases of both configurations with different R and a values. Intersection points in both configurations are given in fig. 4. The values are put in equation (3), and a quadratic equation results.

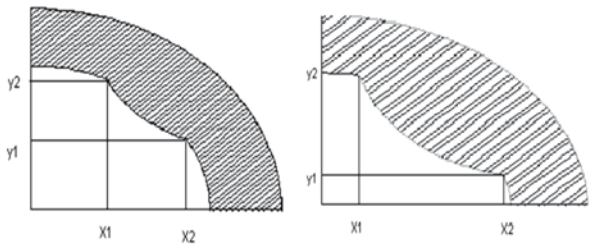

Fig. 4. Intersection points (X1&X2) in rose petal and star grain configuration

2.1.3. Determination of area between the curves using laws of integration

The area between the curves follows from integration given by formula F1.

$$A = \int_{Xa}^{Xb} C1 - \int_{X1}^{X2} C2, \tag{4}$$

The corresponding geometries appear in fig. 5.

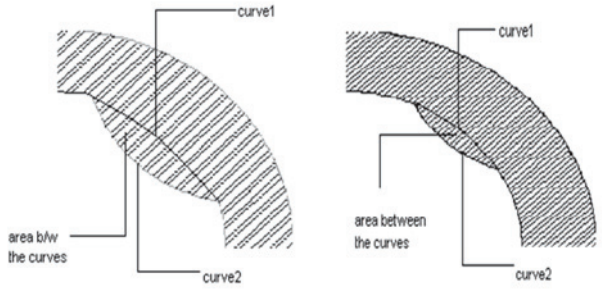

Fig. 5. Area between the curves in star and rose petal grain configuration (in first replica)

The integration of the *circle* equation is given as

$$\int_{xa}^{xb} C1. \tag{5}$$

The integration of the *a* (1/X)* equation is given as

$$\int_{X1}^{X2} C2 = \int_{X1}^{X2} a^*\left(\frac{1}{X}\right)dx,$$

$$\left\{\begin{matrix} X2 \\ X1 \end{matrix} a * \ln X\right\}. \tag{6}$$

In the above section, we have determined limits for both configurations, and by putting these values in formula F1, one gets the area between the curves.

2.1.4. Determining port area

To determine the port area, we find the area of the inner circular curve by using equation (4) and then multiply the answer by 2 (limit of integration with respect to X is (5, -5), as 5 mm is the radius of the inner core of the propellant grain). Now we solve for the following cases.

2.2. Case #1, same port area / burn area for both configurations

Data for both configurations is R=5 mm, a =5 for the star grain configuration and R=5 mm, a =8 for the rose petal grain configuration. By using these data in the equations and formulas given above we are able to calculate the port area. Now to calculate total area, we multiply the area between the curves by the number of star points of the rose petal and star configurations. Here we consider n=4 for both configurations. Hence the area between curves in both configurations is given by

$$T_A = A * n, \tag{7}$$

$$P_A = C_A - T_A. \tag{8}$$

It is evident that the port area of configurations is not equal. For this we have to set an appropriate value of n for both configurations. It comes out that the port area of both configurations is nearly the same if we set n=8 for the rose petal and n=4 for star grain configuration. We however have to determine the circumference bounding the star points to assure that the replication is consistent with constant port area requirements.

The circumference bounding star points are given by formula F5.

$$2 * \begin{Bmatrix} Xb \\ Xa \end{Bmatrix} \left[R * \sin^{-1}\left(\frac{X}{R}\right) \right\}. \tag{9}$$

We have to keep in mind that whatever the value of n, the circumference of the port area should be the same for both grains. We know the limits of the circular arc and star or rose petal arc as shown in fig. 6.

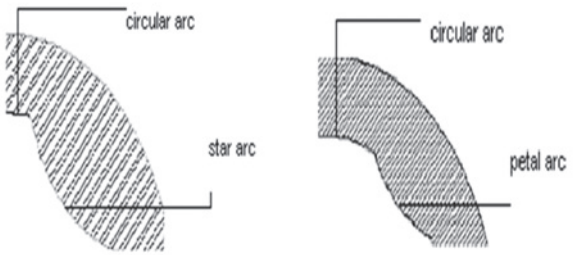

Fig. 6. Arcs in star and rose petal grain configurations (in the first replica)

By putting these limits in the formula (F5) and calculating the circumference of the circular arcs and star or rose petal arcs, we come to know that we have to keep the circumference of the inner curve shape of both configurations constant. For this n can also undergo change. Again for this case n is set as 7 for the rose petal grain configuration, and its value is 4 for the star grain configuration as depicted in fig. 7.

Fig. 7. 7-pointed rose petal grain, 4-pointed star grain (geometry with port area conformity)

2.2.1. Burn area

The formula used for finding burn area is given below.

$$B_A = (L_{C1} + L_{C2}) * L_G. \tag{10}$$

So according to the mathematical formulas

L_{C1}, L_{C2}

The arc length of the *circle curve* is integrated easily *(R asin (X/R))* while the arc length of the *a*(1/x) curve* is not amenable to simple integration. We have to use binomial expansion followed by integration to yield the result:

$$B_A = \begin{Bmatrix} Xb \\ Xa \end{Bmatrix} \left(\left(R \sin^{-1}\left(\frac{X}{R}\right) \right) + \left(-\frac{a}{X} + \frac{1}{6} * \frac{X^2}{a} \right) \right) \Bigg\} * L_G . \tag{11}$$

The thrust, web fraction, and volumetric loading are computed as given below (Sutton, Biblarz 2001; Brooks 1972).

2.2.2. Thrust

Thrust = mass rate *specific impulse
Mass rate= burn area *burn rate*density.
So
Thrust = burn area *burn rate*density *Isp, (12)

2.2.3. Web fraction

The web fraction is given by formula F9
Web fraction = web thickness/radius, (13)

2.2.4. Volumetric loading

To find volumetric loading V_l, the following formulas are executed one by one.

$$A_G = 2 * \int_{-R1}^{R1} \sqrt{(R1^2 - X^2)}\, dx, \tag{14}$$

$$G_V = A_G * L_G, \tag{15}$$

$$P_V = P_A * L_G, \tag{16}$$

$$V_P = G_V - P_V, \tag{17}$$

$$m_p = n * V_P. \tag{18}$$

2.2.5. Sliver calculations

Slivers in actual propellant appear in fig. 8.

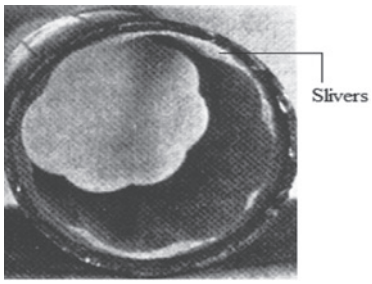

Fig. 8. Depiction of slivers in actual propellant

Sliver area/mass is computed via the following relations

$$S_A = | O_{A1} - O_{A2}| , \quad (19)$$

$$S_A = \left| \int_{Xa}^{Xb} \left(\sqrt{(R1^2 - X^2} - a * \left(\frac{1}{X} \right) \right) 24 \,\&\, dx \right| ,$$

For further calculations we use these formulas given below.

$$S_{TA} = S_A * n, \quad (20)$$

$$S_V = S_{TA} * L_G, \quad (21)$$

$$S_M = n * S_V. \quad (22)$$

2.3. CASE #2, designing rose petal configuration with respect to 6-point star configuration (n=6)

This case is considered because a 6-point star is normally used. Here the rose petal configuration is set according to the 6-point star configuration for the sake of comparison. We have to follow the same procedure as given above. For star grain *R*=6 mm, *a* =12.5 and for rose petal grain *R*=6 mm, *a* =14.6. These calculations show that the 7-pointed rose petal grain configuration shows the same behaviour as the 6-point star grain configuration, with nearly mitigated slivers, as depicted in fig. 9.

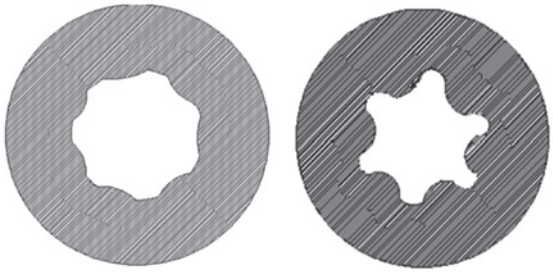

Fig. 9. 7-pointed rose petal grain configuration, 6-pointed star grain configuration

2.4. Programming and computation

In order to perform these mathematical calculations automatically, MATLAB software was used, which helps in generating different curves (thrust – time, burn area – time) for both cases. It also helps in generating the burn patterns. MATLAB is very powerful software that helps in generating powerful two-dimensional and three-dimensional curves. Here programming follows the same module given above.

3. Results and discussions

3.1. Design result analysis

This section includes an analysis of curves generated in MATLAB. Before the analysis of these curves, it is necessary to describe design requirements and constraints.

3.1.1. Design requirements and constraints for both configurations

The thrust – time profile is the primary output. Thrust, pressure, burning time, length, diameter, and mass of propellant determine the design requirements (Khurram *et al.* 2007). In the present study, thrust and burn area have been taken as the objective functions to satisfy the limits on propellant mass, burn time, burn rate, nozzle, propellant parameters, and length and diameters in both grain configurations for comparative analysis. The main system, constraints for current two-dimensional grain design appear in Table 1 (Thomas, Finney 2001; Brooks 1972; Khurram *et al.* 2007).

Table 1. Main system constraints for the current two-dimensional grain design

Requirements and constraints	Values
Length (L_G)(mm)	50
Mass of propellant (m_p)(kg)	Variable
Burn time (t_b)(msec)	Variable
Radius (R)(mm)	12
Throat area (At)(mm^2)	Variable
Thrust coefficient (C_f)	1.54
Burn rate(r)(mm/sec)	1
Port area (P_A)(mm^2)	Variable
Volume of motor (mm^3)	Variable
Density (ρ)(Kg/mm^3)	0 .0000018
Specific impulse (Isp)(s)	240
Web fraction (w_f)	0.35<wf<0.6
Volumetric loading (V_l)	0.7<vl<0.88
Length/diameter (L/D)	NA

3.1.2. Case #1, same port area/burn area in both configurations

In this case, star and rose petal grain configurations are designed for same port area. The star configuration has 4 star points and the rose petal configuration has 7 petal points. For this case, the computed values are given in Table 2.

Table 2. Calculated values of requirements and constraints for case #1

Requirements and constraints	Calculated values
Port area (P_A)(mm²)	53 (star configuration) 55 (rose petal configuration)
Mass of propellant (mp)(Kg)	0.036 (both configurations)
Throat area (At) (mm²)	26.5
Port volume (P_V) (mm³)	2650 (star configuration) 2750 (rose petal grain configuration)
Web fraction (W_f)	0.58 (calculated)
Volumetric loading (Vl)	0.87 (calculated)
Length/diameter (L/D)	NA

3.1.2.1. Burn patterns

Burn patterns of a replica for each configuration are given below in fig. 10. It is seen that complete shape replicates *n* times.

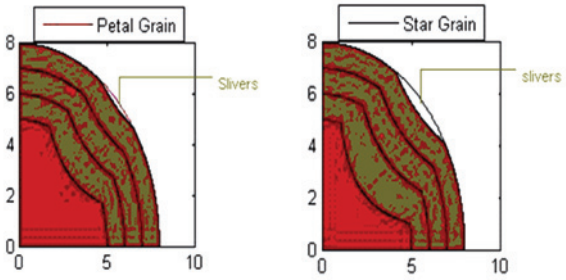

Fig. 10. Burn patterns of rose petal and star grain configurations

3.1.2.2. Output curves

The output thrust and burn area curves for the two configurations appear in Figs 11 and 12.

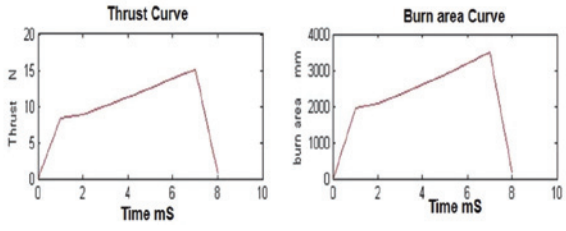

Fig. 11. Rose petal grain thrust and burn area time curves

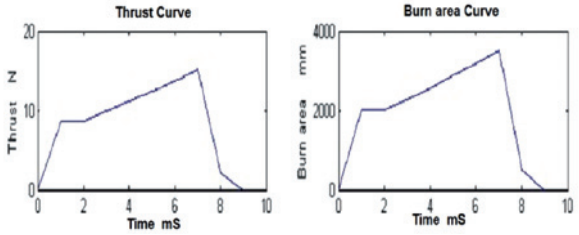

Fig. 12. Star grain thrust and burn area time curves

Comparison of thrust time and burn area time output indicates the following.

From 0 to 1 msec, the curve increases linearly at the commencement of burning for both configurations.

From 1 to 2 msec, the thrust and burn area in the rose petal grain configuration is marginally less than in the star configuration. During this period the curves mimic each other.

From 2 to 7 msec, the thrust and burn area graph increase over time as seen in figure 11 and figure 12.

From 7 to 8 msec, the rose petal grain thrust falls to nearly zero at 8msec. On the other hand, the star grain configuration curve does not fall to zero; the rose petal configuration curve has no tail-off, as opposed to its star counterpart.

From 8 to 9 msec, the star configuration propellant burns at low thrust.

A comparison clearly shows tail-offs in star configuration curves. Tail-offs are negatives showing the portion of wasted propellant that burns at a very low thrust and pressure during the final action time.

3.1.2.3. Case #2, 6-point star with same port area in both configurations

The 6-point star is considered since it is the most used shape. Correspondingly, the rose petal grain configuration is set so that it has 7 petals in a circle with a radius of 6 mm, keeping the port area constant. The calculated values of requirements and constraints appear in Table 3.

Table 3. Calculated values of requirements and constraints for case #2

Requirements and constraints	Calculated values
Port area (P_V)(mm)	100 (star configuration) 99.7 (rose petal configuration)
Mass of propellant (m_p)(Kg)	0.031 (both configurations)
Throat area (At)(mm²)	50 (both configurations)
Port volume (P_V)(mm³)	5000 (both configurations)
Web fraction (W_f)	0.5 (calculated)
Volumetric loading (V_l)	0.78 (calculated)
Length/diameter (L/D)	N.A.

3.1.2.4. Burn patterns

The burn patterns of the two configurations are given below in fig. 13.

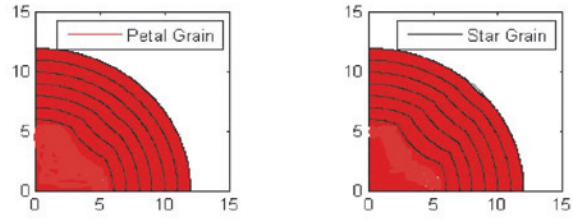

Fig. 13. Burn patterns of petal and star grain configurations

3.1.2.5. Output curves

The output thrust and burn area curves for the two configurations are depicted in Figs 14 and 15.

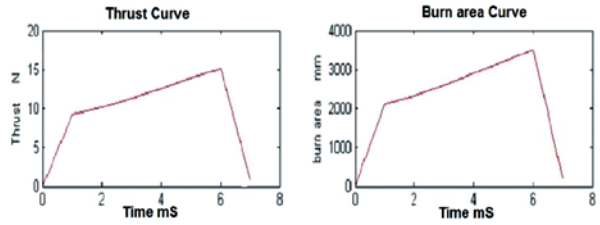

Fig. 14. (7-point) rose petal grain thrust and burn area time curves

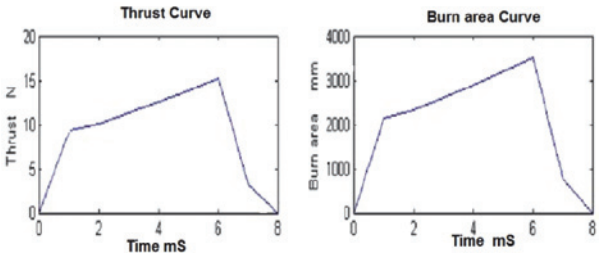

Fig. 15. (6-point) star grain thrust and burn area time curves

From 0 to 1 msec, both curves increase linearly at the commencement of the start of burning.

From 1 to 2 msec, in the star grain configuration, the curve is constant, but for the rose petal grain configuration, the curve is little bit progressive; the values are nearly equal, however.

From 2 to 6 msec, both curves show an increasing trend.

From 6 to 7 msec is an important interval since the rose petal grain curves fall nearly to zero at 7 msec. No tail-offs form thereafter because the propellant has burned completely by this time. On the other hand the star grain configuration curve does not fall to zero.

From 7 to 8 msec, the star configuration propellant burns at low thrust.

One can easily observe the tail-offs of the star grain configuration. It is important to consider the following aspects.

3.1.3. Thrust and burn time

In certain cases, it is desirable to attain required thrust in less burn time to attain high thrust.

Case 1: In this case, both configurations attain same high value of thrust, but the burn time of the star configuration is 9msec as opposed to 8msec for rose petal.

Case 2: Here both configurations attain exactly the same thrust, but the rose petal configuration attains high thrust in less time than the star configuration. The burn time of star grain is more than 8 ms compared with 7 ms for rose petal.

Both configurations attain the same value of thrust, but burn time of the rose petal grain configuration is less than the star grain configuration and, importantly, lacks the attendant sliver tail-off.

3.1.4. Burn area

Both configurations are identical as far as burn area evolution is concerned.

3.1.5. Slivers

Slivers are important for two main reasons. The first one is loss of thrust and the second one is thermal load increase on the motor case during sliver burning (Püskülcü 2004). It is deemed necessary that slivers should be kept at a minimum because useful energy cannot be attained by leftover propellant. That is because leftover propellant burns at very low thrust. Sliver area and unburned mass appear in Table 4.

Table 4. Sliver area and unburned mass for the two configurations

Cases	Sliver area $(mm)^2$	Unburned mass (mg)
Case #1	6.1 (for petal) 9.6 (for star)	549 (for petal) 860 (for star)
Case #2	0.84 (for petal) 10.5 (for star)	75.6 (for petal) 945 (for star)

The comparison given in table 4 between proposed and already existing configurations is crucial. It is observed that in both cases the petal configuration has far less wasted area and unburned propellant mass. On the contrary, the star configuration shows distinct tail-off, with the attendant longer burning duration at lower thrust. This also leads to wastage of propellant. The rose petal configuration is decidedly much better than the star grain configuration from the standpoint of both sliver area and sliver mass. The star grain also shows a much higher fraction of slivers.

3.1.6. Structural integrity

It is necessary to minimise grain failure due to environment, internal pressure, and stresses inside the grain mass. These effects can be minimised by

- reducing web fraction,
- adding other stress features,
- *avoiding sharp curves in the configuration*,
- limiting changes in the port area of grain configuration (Brooks 1972).

A cursory look at the geometry readily reveals that the rose petal is more suitable design when seen in this light. Relatively sharp curves can be seen in the star grain configuration, with higher concentration of stress and higher probability of failure.

4. Conclusion

Novel architecture for a burning surface based on the shape of the rose petal is mathematically modelled and computationally analysed to demonstrate the burn area profile. The new design entails the total mitigation of slivers in the tail-off section, without compromising propulsion system performance as inferred from the thrust time and burn time output. Comparisons are drawn with the established star design, and they clearly exhibit the advantage accrued in the elimination of regressive burning due to slivers. The new design is bound to contribute to more efficient utilisation of solid propellants, which is the most important component of propulsion systems. The aviation industry will gain a boost with this improved propulsion system.

Acknowledgement

Mr. Tahir: lecturer in RCMS (NUST), Islamabad, Pakistan, for assistance in computer programming.

List of Acronyms

SRM Solid rocket motor
EB End burning
STG Slotted tube grain
SG Star grain
AP Ammonium perchlorate
HTPB Hydroxyl-terminated polybutadiene
L Length
D Outer diameter
R Inner radius
n Number of star arcs or rose petal arcs
NA Not applicable
A Area between the curves
C1 Curve1 (circular curve)
C2 Curve 2 (a* (1/X) curve)
Xa, Xb, X1 and X2 intersection points of both curves
T_A Total area between the curves
P_A Port area
C_A Area of inner circle of grain(pi*R^2)
B_A Burn area
L_{C1} Arc length of *circle curve* (curve1)
L_{C2} Arc length of *a* (1/x) curve* (curve2)
L_G Length of grain segment
V_l Volumetric loading
A_G Area of grain segment
R1 Outer radius of grain segment
G_V Grain segment volume
P_V Port volume
V_P Volume of propellant
m_p Mass of propellant
ρ Density
S_A Sliver area
O_{A1} Area of outer circle after complete grain burning
O_{A2} Area of *a*(1/x)* for outer circle after complete burning
S_{TA} Total sliver area
S_V Sliver volume
S_M Mass of slivers

References

Barrere, M. 1977. Analysis of rocket- engine transient regimes, *Acta Astronautica* 44: 641–70. http://dx.doi.org/10.1016/0094-5765(77)90113-8

Brooks, W. T. 1972. *Solid Propellant Grain Design and Internal Ballistics [M]*. NASA SP-8076.

Cai, W; Thakre, P; Yang, V. 2008. A model of AP/HTPB composite propellant combustion in rocket motor environments, *Combust. Sci. and Tech*. 180: 69–2143. http://dx.doi.org/10.1080/00102200802414915

Davenas, A. 1993. *Solid Rocket Propulsion Technology [M]*. New York: Elsevier Science & Technology.

Davenas, A.; Thepenier, J. 1999. Recent progress in the prediction and analysis of solid rocket motors [J], *Acta Astronautica* 44: 61–469. http://dx.doi.org/10.1016/S0094-5765(99)00079-X

Dick, W. A.; Health, M. T.; Fiedlero, R. A., *et al.* 2005. Advanced simulation of solid propellant rockets from first principles [C], *AIAA*. 3990.

Khurram, N.; Guozhu, L.; Peng, X. 2007. Performance prediction and optimization of star configuration for solid rocket motor, in *11th International Space Conference of Pacific Basin Societies*. Beijing, China.

Püskülcü, 2004. Analysis 3-D grain burn back of solid propellant rocket motors and verification with rocket motor test.

Ricciardi, A. 1992. Generalized geometric analysis of right circular cylindrical star perforated and tapered grains [J], *Journal of Propulsion and Power* 8: 51–58. http://dx.doi.org/10.2514/3.23441

Stein, S. D. 2008. *Benefits of the Star Grain Configuration for a Sounding Rocket.* United States Air Force Academy Department of Astronautics, USAFA, CO, 80841.

Sutton, G. P.; Biblarz, O. 2001. *Rocket Propulsion Elements*. 7th ed. John Wiley & Sons, Inc., 417–473.

Thomas, G. B.; Finney, R. L. 1995. *Calculus & Analytic Geometry*. 10th ed. California: Addison-Wesley.

Wilcox, M. A.; Brewster, M. Q.; Tang, K., *et al.* 2005. Solid propellant grain design and burn back simulation using a minimum distance function [C], *AIAA*. 4350.